Gold−Sulfur Bonding in 2D and 3D Self-Assembled Monolayers: XPS Characterization

Marie-Caroline Bourg,† Antonella Badia,‡ and R. Bruce Lennox*

Department of Chemistry, McGill University, 801 Sherbrooke St. W., Montreal, Quebec, Canada, H3A 2K6

Received: October 5, 1999; In Final Form: April 18, 2000

Although self-assembled monolayers (SAMs) of alkylthiols on planar gold (2D SAMs) and on gold nanoparticles (3D SAMs) have been intensely studied, the actual nature of the Au−S bonding remains poorly characterized. Comparison of the X-ray photoelectron spectroscopy (XPS) spectra of 2D and 3D SAMs and "reference" Au(I) complexes, sometimes referred to as Au(I) thiolate polymers, provides detailed insight into this problem. We report high-resolution XPS spectra and Au $4f_{7/2}$ and S $2p_{3/2}$ binding energies (BE) in 2D SAMs, 3D SAMs and the Au(I) thiolate complexes for two short-chain thiols (*n*-C_4SH and *n*-C_5SH). Sulfur $2p_{3/2}$ BE shifts are used to compare the different states of bonding in the SAM systems and the Au(I) complexes and establish that the S atom in the SAM systems bears a charge of about 0.2*e*. The 2D and 3D SAMs exhibit similar XPS characteristics and are both distinguishable from the Au(I) complexes. The origins of the observed BE values are discussed in the context of the nature of the gold substrate and the oxidation state of the chemisorbed sulfur atom. Comparison of ^{13}C NMR chemical shift data and XPS BE data further clarifies the nature of the surface interactions as well as the use of the Au(I) complexes as reference materials.

Introduction

Since the first reports of self-assembled monolayer (SAM) formation using aromatic thiols on a platinum surface[1] and dialkyl disulfides on a gold surface,[2] many studies have been directed toward understanding the structure and the dynamics of SAMs of *n*-alkylthiols (RSH) on gold. The applications of these SAMs are now emerging in different fields such as corrosion inhibition,[3] lithography (microfabrication, microelectronic miniaturization),[4] electronic devices,[5] and biosensors.[6] The surface nature of these SAMs, however, imposes limitations on the types of molecular characterization techniques one can use. We have previously used RSH-coated crystalline gold nanoparticles (3D SAMs), 2−3 nm in diameter, to access otherwise inaccessible, but powerful characterization techniques, such as NMR spectroscopy and differential scanning calorimetry (DSC).[7]

To date, several high-resolution X-ray photoelectron spectroscopy (XPS) studies of the Au/RS SAMs have been reported in the literature,[8−15] but few definitive conclusions are available. We have in particular sought to compare the gold−sulfur bond present in the 2D and 3D SAMs. Because the sulfur in 2D SAMs is widely stated to be in the form of a thiolate,[12,16−18] we also compare the oxidation state of the sulfur and gold in the 2D and 3D SAMs with that in Au(I) complexes (referred to as Au(I) thiolate polymer). Three questions are of particular interest in this regard: (i) is the Au−S bonding the same in the planar (2D) system and the nanoparticles (3D)? (ii) how does the bonding in the SAMs relate to that of the Au(I) complexes? (iii) what do the XPS binding energy (BE) values tell us about the actual Au−S interaction? The first question is of continued interest as the 3D (nanoparticle) system would appear to have many available bonding configurations because of the limited facet size and large number of edge and near-edge surface atoms. The second question arises because this rather incompletely characterized complex has been used as a reference material. The details of the bonding in the complex are not yet well described and indeed Au−alkylthiolate complexes of this type appear to be quite complicated. The third question arises because the origin of BE shifts in adsorbates is in itself complex and requires more than just direct BE comparisons to be meaningful. In this comparative study, we use two short-chain alkylthiols (*n*-C_4SH, *n*-C_5SH) to form SAMs on planar (2D) and nanoparticle (3D) surfaces. Short-chain alkylthiols were chosen for this study because they attenuate the photoelectron yield to a lesser extent than do longer chains[19] and thus allow for excellent spectral signal-to-noise.

^{13}C NMR measurements of the 3D RS/Au systems are very useful in assessing the changes associated with formation of the Au−S bond.[7,20] It is difficult however to definitively assign the origins of ^{13}C chemical shifts in such complex materials. The similar ^{13}C chemical shifts (as in the case of the *n*-C_4S/Au nanoparticles and the *n*-C_4S/Au(I) complex[7]) suggest, but do not firmly establish, a case for equivalent bonding. The factors which control core level binding energies of adsorbates on the nanoparticles (as determined by XPS) are different from the factors which determine ^{13}C chemical shifts. A comparison of data trends from the two techniques may thus allow for more definitive conclusions in the SAM vs reference compound comparison.

Experimental Section

n-C_4SH (99%), *n*-C_5SH (98%), $HAuCl_4 \cdot 3H_2O$, sodium borohydride (99%), tetraoctylammonium bromide (98%), and thiodiglycol (99%) were obtained from Aldrich and were used as received. The alkylthiol purity was monitored by high field ^{1}H NMR (500 MHz) and ^{13}C NMR (125 MHz) spectroscopy.

1. Preparation of the Self-Assembled Monolayers (2D-SAMs). Gold slides (1000 Å thick, Evaporated Metal Films, Utica, USA) were cleaned in a solution of boiling 50% chloroform/50% ethanol. The slides were then washed with a copious quantity of distilled water and ethanol, followed by

* Corresponding author. E-mail: Bruce_Lennox@maclan.mcgill.ca.
† E-mail: Bourg@chemistry.mcgill.ca.
‡ Present address: Université de Montréal, CP 6128, Montreal, QC, Canada, H3C 3J7. E-mail: antonella.badia@umontreal.ca.

10.1021/jp9935337 CCC: $19.00
Published on Web 06/24/2000

sonication in ethanol. They were then incubated in a 0.1 mM alkylthiol/ethanol solution for at least 48 h. The incubated slides were then washed with large quantities of H_2O and ethanol, dried under a N_2 stream, and stored in a sealed vial.

2. Preparation of the Gold Nanoparticles (3D-SAMs). The nanoparticles were synthesized following the procedure of Brust et al.[21] In this procedure, the nanoparticles are formed in a two-phase system. The gold salt, $HAu(III)Cl_4 \cdot 3H_2O$, is dissolved in water and transferred to the alkylthiol/toluene solution via a phase transfer reagent ($(C_8H_{17})_4NBr$). The gold is reduced by $NaBH_4$ in the presence of the thiol surfactant at the toluene−water interface. Upon addition of the reducing reagent, the organic phase changes from orange to deep brown within a few seconds. The reactions were carried out under ambient atmosphere for 3 h. The particles were exhaustively washed with ethanol to remove free thiol and disulfide. The purity of the particles was tested by (i) silica gel TLC using hexanes as the mobile phase and (ii) ^1H NMR (500 MHz; Varian Unity 500) and ^{13}C NMR (125 MHz), where the absence of sharp, alkyl-related peaks is diagnostic of the absence of unbound thiol,[7] at least at the detection level of the NMR experiment. The absence of a S $2p_{3/2}$ peak in the XPS spectra also confirms that the samples do not have unbound thiol chains.[12] The diameters of these nanoparticles are 2.9 ± 0.5 nm for *n*-C_4 and, 2.6 ± 0.4 nm for *n*-C_5 as determined by TEM (see Supporting Information).

3. Preparation of the Gold(I) Complexes. The preparation of the gold(I) complexes was adapted from the procedure of Al-Saady et al.[22] One millimole (0.394 g) of $HAu(III)Cl_4 \cdot 3H_2O$ was dissolved in water (10 mL), and the stirred solution was ice cooled. When the solution neared 0 °C, thiodiglycol (0.366 g, 3.0 mmol) was added. The solution immediately became colorless, after which the alkylthiol was introduced from a syringe in a dropwise fashion. A yellowish-white powdery precipitate was formed and the reaction was continued for an additional 5 min. The product was isolated by vacuum filtration and exhaustively rinsed with Millipore water (6×25 mL) and finally freeze-dried.

Two other preparation methods were used to prepare the C_5S/Au(I) complex. The first is as per McNeillie et al.,[23] and the second involves two-phase conditions[21] but uses neither a phase transfer agent nor a reducing agent. The product of each procedure yielded materials with equivalent solid state ^{13}C NMR spectra.

4. X-ray Photoelectron Spectroscopy. XPS experiments were conducted using a VG ESCALAB 220i-XL spectrometer employing a monochromatic Al Kα X-ray source ($h\nu = 1486.6$ eV) and a hemispherical electrostatic analyzer. The analysis chamber was always maintained below 10^{-9} Torr. Binding energies (BE) are referenced to the C 1s of alkyl chains or alkyl contaminants at 284.6 eV. The high-resolution Au 4f, S 2p, and C 1s spectra were acquired with a constant analyzer pass energy scan of 20 eV. All the samples have been examined in duplicate. Powders which exhibited excessive charging were pressed into pellets with graphite to reduce the charging; this also improves the resolution of the peaks. The BE is referenced to the C 1s of graphite at 284.5 eV when samples were mixed with graphite. A flood gun was used to minimize charging when necessary. Spectral curve fitting was performed with the Origin peak-fitting module software (Microcal Origin, version 5.0). The gold peaks were fitted using the Voight function.[25] The S 2p peaks were fitted using a Gaussian function with provision for the 1.2 eV spin−orbit splitting of the $2p_{1/2}$ and $2p_{3/2}$; the 1:2 intensity ratio of this splitting was maintained in the fitting. The number of atoms of the element A probed is proportional to the intensity of the normalized peak divided by the sensitivity factor of the element A for the corresponding transition. As a result, the elemental ratio (A to B) is accessed using

$$n_A/n_B = (I_A S_B)/(I_B S_A)$$

where S_A is the sensitivity factor of the element A for the main photopeak. S_A is the product of the cross section (σ_A) and the transmission factor of the electron energy analyzer (T_A) of the element A.

It is well established that long-chain SAMs measurably attenuate photoelectron peak intensities.[19] To evaluate whether attenuation factors in our quantitative analysis are necessary, we compared the intensities of the gold peaks of the *n*-C_4SH and *n*-C_5SH SAMs on gold slides to a clean gold slide used as a reference. The peak intensities for short-chain RS/Au were, in fact similar to, or greater than, the peak intensity of the clean gold. The "bare" gold as measured has surface carbon and oxygen contaminants that attenuate the photoelectron yield to an even greater extent than do the C_4 and C_5. For this reason and the fact that the attenuation problem will be minimal for these short chains, we do not use an attenuation correction in the determination of elemental composition ratios.

5. NMR Spectroscopy. Solution NMR (^{13}C, ^1H) spectra of the nanoparticles were obtained using a JEOL ECLIPSE-270 or a Varian Unity 500 spectrometer at room temperature. Thirty to forty mg of each sample was dissolved in d_6-benzene. For the insoluble Au(I) complexes, solid state NMR was used. ^{13}C CPMAS NMR spectra were obtained at 75.34 MHz using a CheMagnetics CMX-300 spectrometer. Samples were placed in 7.5 mm zirconia rotors and spun at 3−4 kHz. The contact time and recycle delay were 2 ms and 2 s, respectively. Typically several hundred to several thousand transients were collected per spectrum.

6. Data Handling/Fitting. The XPS spectrometer employed in this study is capable of high-resolution measurements (fwhm of 0.6 eV for Ag) that enable us to accurately analyze small shift differences. The positions of the gold and sulfur peaks in the 2D and 3D SAMs and the Au(I) complexes are reproducible to within ±0.1 eV. Each sample was measured until the difference in BE shifts of two measurements was less than 0.1 eV. The values reported in Table 1 are the mean of two experiments. C 1s and S 2p high-resolution scans were run in

TABLE 1: XPS Data of RS/Au Systems

	binding energy (eV)			elemental ratios	
	Au $4f_{7/2}$[a]	S $2p_{3/2}$[a]	C 1s[a]	Au/S[b]	C/S[c]
		n-C_4			
2D-SAMs	83.9	162.0	284.6	23.0	4.4
3D-SAMs	83.8	162.1	284.6	3.5	5.1
Au(I) complex[d]	84.4	162.7	284.6	0.9	3.7
		n-C_5			
2D-SAMs	84.0	162.0	284.6	25.0	5.1
3D-SAMs	83.8	162.1	284.6	3.2	5.3
Au(I) complex	84.2	162.5	284.6[e]	1.0	8.7[e]

[a] Binding energy values for principal elements in eV; referenced to aliphatic carbon. [b] Au to S atom ratio obtained using peak intensities and sensitivity factors as per text. [c] C to S atom ratio obtained using peak intensities and sensitivity factors as per text. [d] A *t*-C_4S/Au(I) complex was also prepared and gave very similar data. SAMs prepared from the *t*-C_4SH gave variable results, however, most probably reflecting inherent instability because of packing constraints. [e] Average of two experiments, one with graphite matrix and one without. Values reported for the C 1s shift and the carbon-to-sulfur ratio corresponds to the nongraphite experiment.

duplicate for each sample (at the beginning and the end of the experiment). No discernible changes were observed, consistent with there being no observable beam damage during the course of the 15 min experiment. This is significant given that beam damage and spectrometer-mediated chemical transformations can greatly complicate sulfur-oriented XPS studies. This is the case in classic bioinorganic/complex studies[26,27] and is a persistent concern in RS/Au SAM studies.[28]

Basic photoelectron peaks have a Lorentzian shape, but instrumental factors and factors associated with the sample (such as phonon broadening) introduce a Gaussian contribution to the line shape. The Voight function[25] is a convolution of a Lorentzian and a Gaussian and is often used for XPS spectral fittings. The final peak shape is usually asymmetric due to various loss processes, such as plasmon peaks, inelastically scattered electrons, satellites, and interaction of the photoelectron with the conduction band in the case of conductors.[25] The combination of all these processes can result in a tail function on the low kinetic energy (high binding energy) side of a photoelectron peak. Good quality fits to the data were obtained with the Voight function and appropriate background subtraction. It was thus unnecessary to add a tail function to achieve a good fit to the experimental data. A straight-line background subtraction has been used for carbon and a Boltzmann line background subtraction has been used for gold and sulfur.

Results and Discussion

In all of the 2D and 3D SAMs studied, the Au $4f_{7/2}$ BE values correspond to Au(0) (83.9 ± 0.1 eV, Figures 1 and 2, Table 1). There is neither a Au(I)-associated peak nor is there evidence for two or more states of Au; the Au $4f_{7/2}$ spectra are notably narrow (fwhm $\sim$ 0.6 eV). The Au $4f_{7/2}$ BE in the Au(I) complexes, however, is shifted by $+0.3 \pm 0.1$ eV with respect to the Au(0) position. The direction of this shift clearly corresponds to Au being in an oxidized state, and its magnitude is similar to that observed for other Au(I) complexes.[23,29]

The sulfur S $2p_{3/2}$ BE values (Figure 1 and 2, Table 1) are 162.0 eV for both the 2D and 3D SAMs, in agreement with previous 2D SAM reports.[8,12,30] This shift corresponds to a negative charge-bearing S adsorbed on a metal, given that elemental S (S_8) has an S $2p_{3/2}$ BE of 164.2 eV.[31] The S $2p_{3/2}$ BE in the Au(I) complexes is slightly more positive than that of the SAMs (162.6 ± 0.1 eV). It is clear that these shifts are due to neither free alkylthiols nor disulfides, whose expected BE are >163 eV,[32] nor oxidized S, as in sulfoxides or sulfones. Each of these exclusions is significant. Free alkylthiol would arise from an incompletely cleaned or decomposed Au/RS nanoparticle preparation. Disulfide would arise from a synthesis-related contaminant, spectrometer-induced damage,[28] or a surface-mediated process.[33] Sulfones or sulfoxides would arise from reactions related to spectrometer water.[27] The Au:S ratio also excludes this possibility as the Au(I) complexes (and their variants) invariably involve a 1:1 Au:S stoichiometry.[34−36] The Au:S ratio (Table 1) in the Au(1) complexes is consistently very close to 1, as per the previously reported elemental analysis.[7]

The Au:S ratio shows that about 23 Au atoms to each S are measured in the 2D SAMs and about 3 Au to each S in the 3D SAMs. Evidently all of the atoms in the nanoparticles are being reported in the XPS experiment. The C:S ratio in both the 2D and 3D SAMs is close to 4:1 (C_4) and to 5:1 (C_5). Taken together, these data provide evidence that all the observed chains are surface-associated in these samples and that carbon−sulfur bond cleavage is not occurring. Other reports of related samples reflect C−S cleavage,[37] probably reflecting differences in instrument design and beam flux.

A spherical nanoparticle 2.8 nm in diameter (corresponding to about 500 atoms[37]) has about 48% of its gold atoms at the surface. For the more realistic truncoctahedron shape, Au_{140} and Au_{1289} have 68% and 37% of their gold atoms, respectively, at the surface. Thus, if all the surface gold atoms involved in Au−S bonding exist as Au(I), then a peak at 84.3 eV should be prominent.[21,23] In fact, this is not the case, as neither a shoulder, nor peak broadness, nor a shift positive from Au(0) (84.0 eV) is observed.

Several factors may combine to cause the Au $4f_{7/2}$ BE shift to report only Au(0). XPS can indeed differentiate between surface and bulk atoms of noble metals in clusters. The BE of clean gold surface atoms is shifted by as much as −0.4 eV compared to bulk atoms.[38] The same phenomenon has been observed for W 4f BE values, with a shift of −0.35 eV.[39] A second factor could counteract such a negative BE shift. The BE values of variable-size metal clusters become more positive compared with the bulk, as the particle size decreases.[40] This trend was demonstrated for the specific case of gold, where bulklike properties in gold clusters occur in the >100−200 atom range.[41,42] The nanoparticles in this study are larger (>350 atoms), suggesting that this size factor is probably not significant here. Charging can also lead to positive BE shifts. However, the particles measured here are clearly metallic given that in the XPS experiment they do not express the charging characteristic of insulating materials. The null or small negative Au $4f_{7/2}$ BE shift could thus arise from a combination of the surface atoms having a shift to lower BE (of up to −0.4 eV); cf. bulk atoms and the oxidized state of the gold causing a counteracting shift to a higher BE (up to +0.3 eV). The net effect is a fortuitous positioning of the Au $4f_{7/2}$ XPS peak at, or near, the shift of bulk Au(0). Although these surface and oxidation state effects could also arise in the 2D SAMs, it is unlikely that they will be observable. Even if the Au(surface):S ratio is 3:1, a Au(I) peak at 84.3 eV would make up only about 5% of the integrated Au $4f_{7/2}$ intensity given that the Au:S integrated ratio is 23:1.[41] Such a peak would be indiscernible with the resolution of our instrument.

The S $2p_{3/2}$ BE values can in fact be related to the charge density on the S atom, as was demonstrated in the classic work of Siegbahn and co-workers.[43] This work presented a linear free energy relationship LFER (S $2p_{3/2}$ BE vs calculated charge, q) based on 132 organic sulfur compounds ranging from thiolates to sulfonium ions. The S $2p_{3/2}$ BE values reported in Table 1 clearly correspond to partially reduced sulfur species. These principles have been recently confirmed in a recent work[44] describing 12 additional gold complexes. Another useful comparison is to metal sulfides (NiS_x, Li_xMoS_y, and Au_2S) which have S $2p_{3/2}$ BE values of 161.1−162.2 eV.[45,46] Interpolation of the data in Table 1 into the Siegbahn LFER suggests that the S in the 2D and 3D Au/SR SAMs bears a charge of $-0.2e$.[47] Porter and co-workers have very recently arrived at the same conclusion for the 2D case.[16] Ab initio calculations of 2D SAMs have predicted that the degree of discrete charge buildup on the S depends on the type of adsorption site adopted ($-0.4e$ for hollow site or $-0.7e$ for top site).[18] An experimentally derived value for the charge of $-0.2e$ per S thus establishes that the Au−S bond is thiolate-like, with extensive covalent character.

Although the alkylthiol RS Au complexes are used as reference materials, they are not, in fact, especially well characterized. Comparison to related systems (i.e., (*i*-propyl)$_3$PhSAu[34,48] and AgRS[49] suggests that the AuRS complex

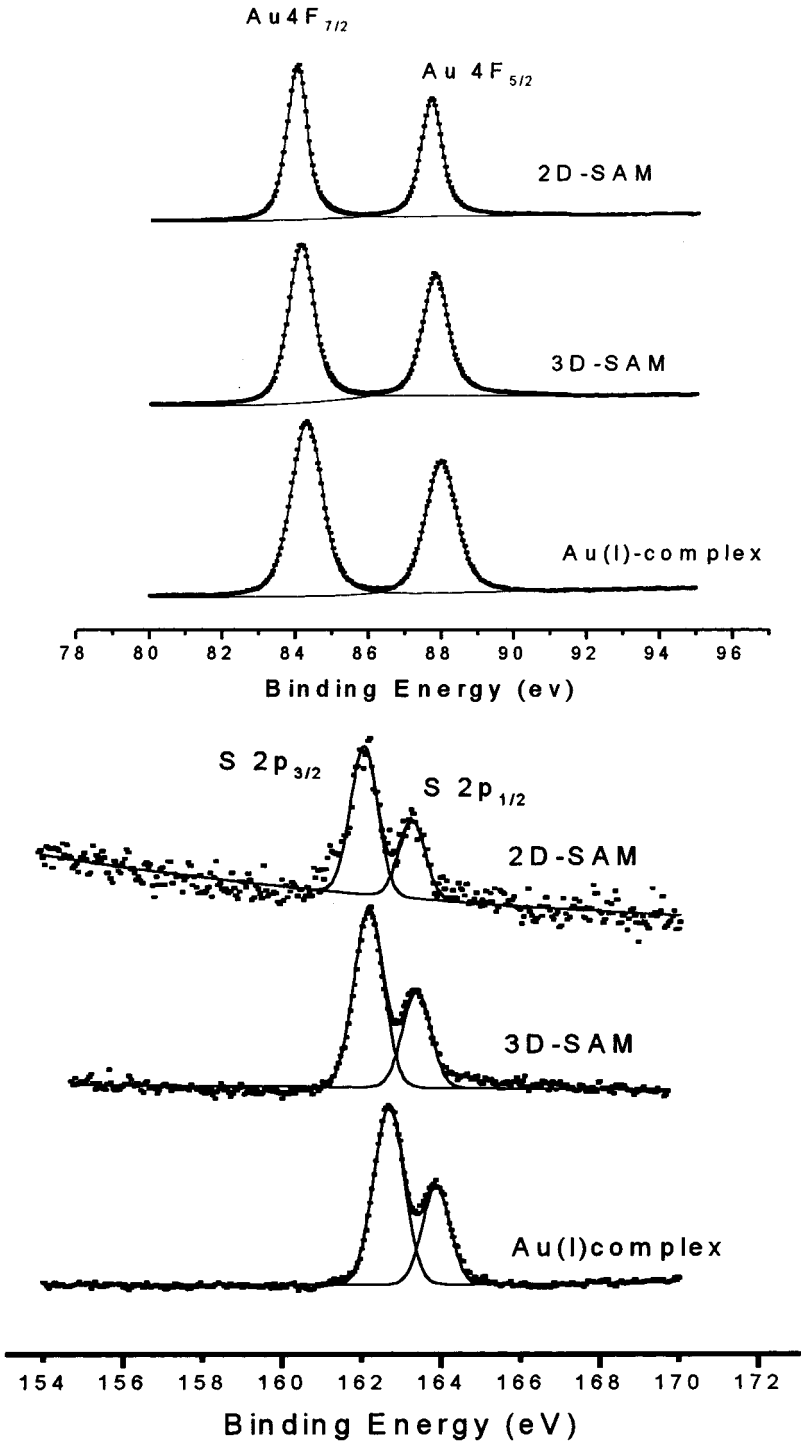

Figure 1. XPS spectra of *n*-butanethiolate (*n*-C_4SH) for 2D SAMs, 3D SAMs, and Au(I) complex. Au 4f (top) and S 2p (bottom).

may involve polymeric chains or rings. The S $2p_{3/2}$ BE in the Au(I) complexes is 162.6 ± 0.1 eV; this corresponds to a net charge of $\sim -0.1e$ on the sulfur.[47] In general, the bridging S in M−S(R)−M complexes (M = Au, Ag, Ni, Pd or Pt) exhibits higher S $2p_{3/2}$ BEs (i.e., less reduced) than the values observed here.[36] The S in M−S(R)−M complexes is likely to involve at least two types of bonding interactions with gold, resulting in a lessening of the extent of negative charge residing on the S atom.

Solid state ^{13}C spectra[7a] of both the nanoparticles and the Au(I) complex exhibit substantial downfield shifts of the C1 peak and a modest shift of the C2 peak cf. the simple alkylthiolate (Na^+RS^-). Electronic conduction band effects (Knight shift) on the ^{13}C NMR shifts have been shown to be unimportant in the nanoparticles. The solid state C1 chemical shifts of the $Na^+C_4S^-$ salt, 3D SAM, and Au(I) complex (chemical shifts of 26.2, 46.5, and 40.1 ppm) suggest that the bonding in the 3D SAM and Au(I) complex are quite different from that of the sodium thiolate but may indeed be similar to one another.[7] The XPS data in Table 1 confirms the similarities in bonding suggested by NMR spectroscopy, as the S in the 3D (and 2D) SAMs is indeed in a reduced state similar to that in the Au (I) complexes. The combination of NMR and XPS experiments thus reveals considerable information about the Au−S bonding in 3D (and by inference, 2D) SAMs.

XPS does not directly establish the oxidation state of the

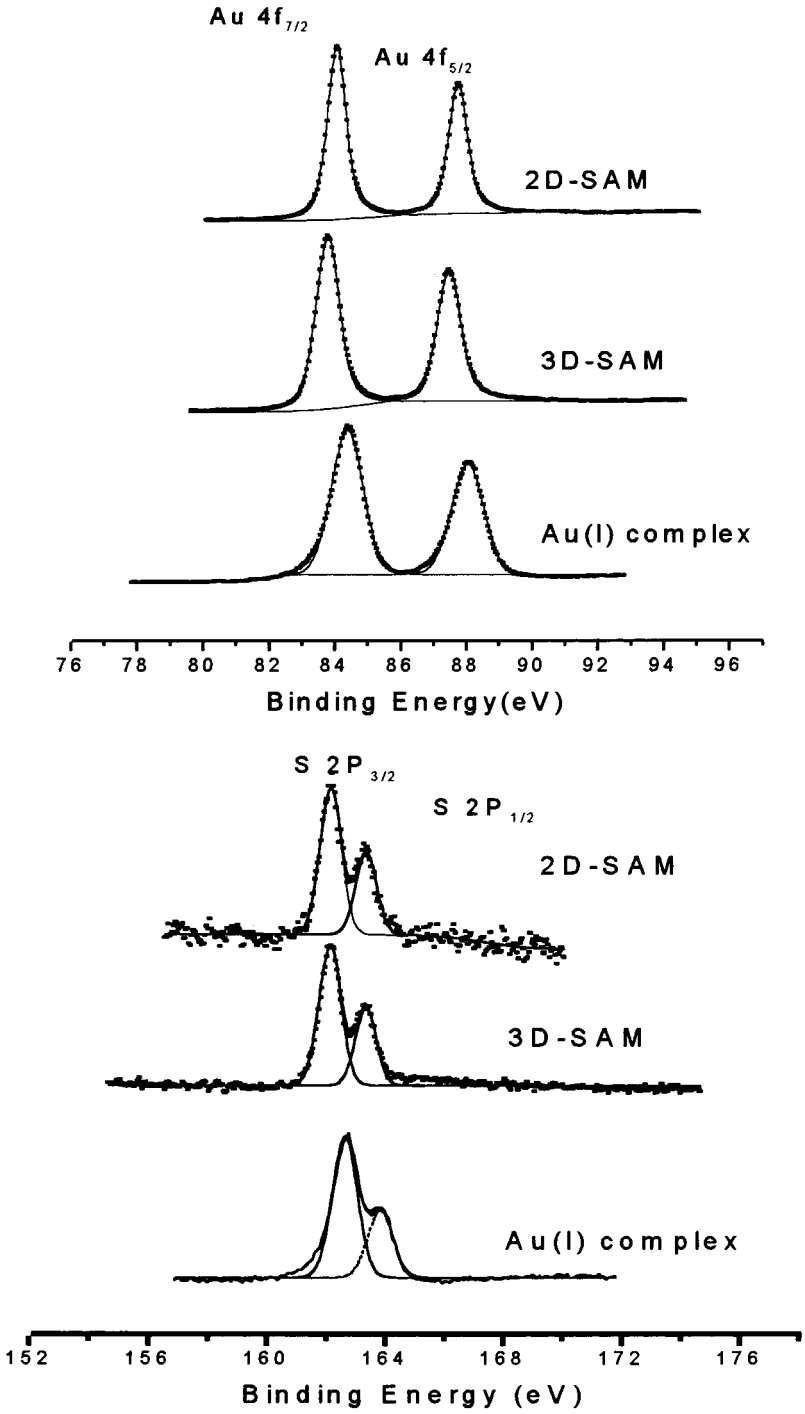

Figure 2. XPS spectra of *n*-pentanethiol (*n*-C_5SH) for 2D SAMs, 3D SAMs, and Au(I) complex. Au 4f (top) and S 2p (bottom). Some charging effects are observed at the low BE foot of the Au(I) complex peak.

surface gold atoms for resolution and surface reasons. Evidence is presented, however, that the corresponding sulfur is in a reduced state in both 2D and 3D SAMs and that the charge per S is about $-0.2e$. The S $2p_{3/2}$ BE data thus provide the best evidence to date that the gold is indeed partially oxidized and that the gold−sulfur bond has a significant covalent character in both 2D and 3D SAMs.

Conclusions

XPS spectra establish that the Au−S bonding in 2D and 3D RS/Au SAMs is essentially the same. The close relationship between bonding in the 2D and 3D SAMs confirms that the high surface area 3D SAM system can be used to probe properties of SAMs by both bulk and surface spectroscopic techniques. The sensitivity restrictions inherent in the 2D SAM systems can thus be circumvented by using the 3D SAMs. The complete alkyl chain remains attached to the surface and no measurable degree of S−C cleavage occurs in either system during measurement. For both 2D and 3D SAMs, a combination of there being only a small proportion of surface Au atoms, surface effects on the BE, and the actual oxidation state all conspire to report a Au $4f_{7/2}$ BE shift which corresponds to the Au(0) state. The alkylthiol sulfur however is in a measurably reduced state, where the partial charge on the S is estimated to be about $-0.2e$. Because the widely used Au(I) reference complexes and the 3D RS/Au SAMs have similar XPS and

NMR signatures, we conclude that the nature of the bonding is indeed quite similar in these systems. We anticipate that ongoing electrochemical and ultraviolet photoelectron spectroscopy studies will provide further insight into the bonding of these interesting systems.

Acknowledgment. We thank Georges Veilleux and Dr. Roy Paynter (INRS-Varennes) for helpful discussions and NSERC (Canada) for financial support of this research.

Supporting Information Available: Figures 1 and 2 show the size distribution of *n*-C_5 and *n*-C_4 nanoparticles; a description of TEM experiments is also given. This material is available free of charge via the Internet at http://pubs.acs.org.

References and Notes

(1) Soriaga, M. P.; Hubbard, A. T. *J. Am. Chem. Soc.* **1982**, *104*, 3937−3945.

(2) Nuzzo, R. G.; Allara, D. L. *J. Am. Chem. Soc.* **1983**, *105*, 4481−4483.

(3) Jennings, G.; Munto, J. C.; Yong, T.-H.; Laibinis, P. E. *Langmuir* **1998**, *14*, 6130−6140.

(4) Xia, Y.; Whitesides, G. M. *Angew. Chem., Int. Ed. Engl.* **1998**, *37*, 550−575.

(5) Vondrak, T.; Zhu, X. Y. *J. Phys. Chem. B* **1999**, *103*, 4892−4899.

(6) Duschl, C.; Liley, M.; Corradin, G.; Vogel, H. *Biophys. J.* **1994**, *67*, 1229−1237.

(7) (a) Badia, A.; Demers, L.; Dickinson, L.; Morin, F. G.; Lennox, R. B.; Reven, L. *J. Am. Chem. Soc.* **1997**, *119*, 11104−11105. (b) Badia, A.; Demers, L.; Cuccia, L.; Lennox, R. B. *J. Am. Chem. Soc.* **1997**, *119*, 2682−2692. (c) Badia, A.; Singh, S.; Demers, L.; Cuccia, L.; Brown, G. R.; Lennox, R. B. *Eur. J. Chem.* **1996**, *2*, 359−363.

(8) Bain, C. D.; Biebuyck, H. A.; Whitesides, G. M. *Langmuir* **1989**, *5*, 723−727.

(9) Weisshaar, D. E.; Walczak, M. M.; Porter, M. D. *Langmuir* **1993**, *9*, 323−329.

(10) Walczak, M. M.; Alves, C. A.; Lamp, B. D.; Porter, M. D. *J. Electroanal. Chem.* **1995**, *396*, 103−114.

(11) Zubragel, C.; Deuper, C.; Schneider, F.; Neumann, M.; Grunze, M.; Schertel, A.; Woll, C. *Chem. Phys. Lett.* **1995**, *238*, 308−312.

(12) Castner, D. G.; Hinds, K.; Grainger, D. W. *Langmuir* **1996**, *12*, 5083−5086.

(13) Rieley, H.; Price, N.; Smith, T. L.; Yang, S. *J. Chem. Soc., Faraday Trans.* **1996**, *92*, 3629−3634.

(14) Hostetler, M. J.; Wingate, J. E.; Zhong, C.-J.; Harris, J. E.; Vachet, R. W.; Clark, M. R.; Londono, J. D.; Green, S. J.; Stokes, J. J.; Wingnall, G. D.; Glish, G. L.; Porter, M. D.; Evans, N. D.; Murray, R. W. *Langmuir* **1998**, *14*, 17−30.

(15) Bensebaa, F.; Zhou, Y.; Deslandes, Y.; Kruus, E.; Ellis, T. H. *Surf. Sci.* **1998**, *405*, L472−L476.

(16) Zhong, C.-J.; Brush, R. C.; Anderegg, J.; Porter, M. D. *Langmuir* **1999**, *15*, 518−525.

(17) Zhong, C.-J.; Zak, J.; Porter, M. D. *J. Electroanal. Chem.* **1997**, *421*, 9−13.

(18) Sellers, H.; Ulman, A.; Shindman, Y.; Eilers, J. E. *J. Am. Chem. Soc.* **1993**, *15*, 9389−9401.

(19) Bain, C. D.; Whitesides, G. M. *J. Phys. Chem.* **1989**, *93*, 1670−1673.

(20) The C1 chemical shift in C14/Au nanoparticles is 42 ppm and in the Au(I) C14S is 40.1 ppm.

(21) Brust, M.; Walker, M.; Bethell, D.; Schiffrin, D. J.; Whyman, R. *J. Chem. Soc., Chem. Commun.* **1994**, *7*, 801−802.

(22) Al-Saady, A. K.; McAuliffe, C. A.; Parish, R. V.; Sandbank, J. A. *Inorganic Syntheses*; John Wiley & Sons: New York, 1985.

(23) McNeillie, A.; Brown, D. H.; Smith, W. E. *J. Chem. Soc., Dalton. Trans.* **1980**, 767−770.

(24) Brust, M.; Fink, J.; Bethell, D.; Schiffrin, D. J.; Kiely, C. J. *J. Chem. Soc., Chem. Commun.* **1995**, 1655−1656.

(25) Briggs, D.; Seah, M. P. *Practical Surface Analysis*, 2nd ed.; John Wiley & Sons: New York, 1996; Vol. 1.

(26) Thompson, M.; Whelan, J.; Zemon, D. J.; Bosnich, B.; Salomon, E. I.; Gray, H. B. *J. Am. Chem. Soc.* **1979**, *101*, 2482−2483.

(27) Thompson, M.; Zemon, D. J.; Lennox, R. B. *Anal. Chem.* **1979**, *51*, 2260−2263.

(28) Zerulla, D.; Chasse, T. *Langmuir* **1999**, *15*, 5285−5294.

(29) We have also considered the possibility that this shift has a charging component. We do not believe that this is a factor here, given that the samples were analyzed in a conducting graphite matrix and that when a flood gun was used, changes to lower BE values did not occur.

(30) Evans, S. D.; Goppert-Berarducci, K. E.; Urankar, E.; Gerenser, L. J.; Ulman, A. *Langmuir* **1991**, *7*, 2700−2709.

(31) Riga, R.; Verbist, J. J. *J. Chem. Soc., Perkin Trans. 2* **1983**, *10*, 1545−1551.

(32) Bourg, M.-C.; Lennox, R. B. Unpublished results.

(33) Sandroff, C. J.; Herschbach, D. R. *J. Phys. Chem.* **1982**, *86*, 3277−3279.

(34) Schröter, I.; Strähle, *J. Chem. Ber.* **1991**, *124*, 2161−2164.

(35) Leblanc, D. J.; Smith, R. W.; Wang, Z.; Howard-Lock, H. E.; Lock, C. J. L. *J. Chem. Soc., Dalton Trans.* **1997**, 3263−3267.

(36) Walton, R. A. *Coord. Chem. Rev.* **1980**, *31*, 183−220.

(37) Whetton, R. L.; Khoury, J. T.; Alvarez, M. M.; Srihari, M.; Vezmar, I.; Wang, Z. L.; Stephens, P. W.; Cleveland, C. L.; Luedtke, W. D.; Landman, U. *Adv. Mater.* **1996**, *8*, 428−433.

(38) Citrin, P. H.; Werthein, G. K. *Phys. Rev. B* **1983**, *27*, 3160−3175.

(39) van der Veen, F. F.; Eastman, D., E.; Bradshaw, A. M.; Holloway, S. *Solid State Commun.* **1981**, *39*, 1301−1304.

(40) Citrin, P. H.; Wertheim, G. K. *Phys. Rev. B* **1983**, *27*, 3176−3200.

(41) Masson, M. G. *Cluster Models for Surface and Bulk Phenomena*; Pacchioni, G., et al., Eds.; Plenum Press: N.Y., 1992; Vol. 283, pp 115−129.

(42) There is a difference in the Au/S stoichiometry in 3D SAMs (2:1) cf. 2D SAMs (3:1). A combination of 3:1, 2:1, and 1:1 Au−S binding is necessary to fulfill the range of Au/S ratios (1.55−1.87) calculated by Luedtke et al. (*J. Phys. Chem.* **1996**, *100*, 13324−13329). The XPS experiments reported here cannot, however, resolve these different binding combinations.

(43) Lindberg, B. J.; Hamrin, G. J.; Gelius, U.; Fahlman, A.; Nordling, C.; Siegbahn, K. *Phys. Scr.* **1970**, *1*, 286−298.

(44) Nakamoto, M.; Mashida, A. *Kagatuto Kogyo* **1998**, *72*, 424−430.

(45) Khudorozhko, G. F.; Asanov, I. P.; Mazalov, L. N.; Kravtsova, E. A.; Parygina, G. K.; Fedorov, V. E.; Mironov, J. V. *J. Electron Spectrosc. Relat. Phenom.* **1994**, *68*, 199−209.

(46) Rodriguez, J. A.; Li, S. Y.; Hrbek, J.; Huang, H. H.; Xu, G.-Q. *Surf. Sci.* **1997**, *370*, 85−95.

(47) When corrected for the choice of carbon reference and the S $2p_{3/2}$/$2p_{1/2}$ splitting, the Siegbahn LFER for sulfur describes a relationship where $BE = 4.75q + 163.03$ eV, ($r = 0.9733$), where q is the net charge on the S. This LFER is based on organosulfur compounds.

(48) LeBlanc, D. J.; Britten, J. F.; Wang, Z.; Howard-Lock, H. E.; Lock, C. J. L. *Acta Crystallogr. C* **1997**, *C53*, 1763−1765.

(49) Dance, I. G.; Fitzpatrick, L. J.; Rae, A. D.; Scudder, M. L. *Inorg. Chem.* **1983**, *22*, 3785−3788.